Biogeosciences Discuss., 10, 6417–6459, 2013
www.biogeosciences-discuss.net/10/6417/2013/
doi:10.5194/bgd-10-6417-2013

Biogeosciences
Discussions
Open Access

Productivity of aboveground coarse wood biomass and stand age related to soil hydrology of Amazonian forests in the Purus-Madeira interfluvial area

B. B. L. Cintra[1,2], J. Schietti[1], T. Emillio[1], D. Martins[1], G. Moulatlet[1], P. Souza[1], C. Levis[1], C. A. Quesada[1], and J. Schöngart[1,2]

[1]Instituto Nacional de Pesquisas da Amazônia (INPA), Manaus, Amazonas, Brazil
[2]Max Planck Institute for Chemistry, Biogeochemistry Department, Mainz, Germany

Received: 6 January 2013 – Accepted: 13 March 2013 – Published: 5 April 2013

Correspondence to: B. B. L. Cintra (biomail.bruno@gmail.com)

Published by Copernicus Publications on behalf of the European Geosciences Union.

Abstract

The ongoing demand for information on forest productivity has increased the number of permanent monitoring plots across the Amazon. Those plots, however, do not comprise the whole diversity of forest types in the Amazon. The complex effects of soil, climate and hydrology on the productivity of seasonally waterlogged interfluvial wetland forests are still poorly understood. The presented study is the first field-based estimate for tree ages and wood biomass productivity in the vast interfluvial region between the Purus and Madeira rivers. We estimate stand age and wood biomass productivity by a combination of tree-ring data and allometric equations for biomass stocks of eight plots distributed along 600 km in the Purus-Madeira interfluvial area that is crossed by the BR-319 highway. We relate stand age and wood biomass productivity to hydrological and edaphic conditions. Mean productivity and stand age were $5.6 \pm 1.1\,\mathrm{Mg\,ha^{-1}\,yr^{-1}}$ and 102 ± 18 yr, respectively. There is a strong relationship between tree age and diameter, as well as between mean diameter increment and mean wood density within a plot. Regarding the soil hydromorphic properties we find a positive correlation with wood biomass productivity and a negative relationship with stand age. Productivity also shows a positive correlation with the superficial phosphorus concentration. In addition, superficial phosphorus concentration increases with enhanced soil hydromorphic condition. We raise three hypotheses to explain these results: (1) the reduction of iron molecules on the saturated soils with plinthite layers close to the surface releases available phosphorous for the plants; (2) the poor structure of the saturated soils creates an environmental filter selecting tree species of faster growth rates and shorter life spans and (3) plant growth on saturated soil is favored during the dry season, since there should be low restrictions for soil water availability.

1 Introduction

The increased number of permanent plots in the recent years has contributed to improve the understanding of regional variation in forest productivity across the Amazon Basin (Baker et al., 2004; Malhi et al., 2004; Giardin et al., 2010). The use of adjusted allometric models for different regions (Chave et al., 2005; Feldpausch et al., 2012) contributed to more reliable estimates on biomass storage and productivity in Amazonian forests. However, the existing studies do not cover the full range of forest ecosystems across the Amazonia. Most of the studies on wood biomass production focus on non-flooded terra firme forests. Few studies focus on wooded wetlands seasonally flooded by large rivers, but other types of wooded wetlands remain mostly overlooked. In the Amazonia, wetlands constitute about 30 % of the total area (Junk et al., 2011), of which old fluvial terraces located in interfluvial areas not flooded by large rivers cover a large portion. Little is known about environmental factors such as soil conditions, climate and hydrology controlling wood biomass productivity in these interfluvial wetlands.

It has been shown that in non-flooded terra firme forests wood biomass productivity negatively responds to severe droughts such as in 2005 and 2010 (Phillips et al., 2009; Corlett et al., 2011; Lewis et al., 2011). In seasonally flooded forests (várzeas and igapós), on the other hand, an enhanced tree growth can be attributed to El Niño-induced droughts, since the flooded period in El Niño years is shorter than in other years (Schöngart et al., 2004; Schöngart and Junk, 2007). There is also evidence that variations in productivity are related to soil fertility in both terra firme and floodplain forests (Malhi et al., 2004; Schöngart et al., 2005) which consequently results in different stand ages (Schöngart et al., 2010) and biomass stocks (Malhi et al., 2004, 2006). However, interfluvial wetlands present conditions different both from the terra firme and the large river floodplains. As terra firme forests are not homogeneous over the Amazon basin, wetland forests also show considerable variation in structure and functioning.

Interfluvial wetlands are found along vast regions in the central and western Amazonia (Sombroek, 2000). In these regions the water table is shallow and the soils are poorly drained and seasonally waterlogged, presenting a patchwork of seasonally flooded, saturated or non flooded areas. Flooding or saturation may occur by pooling of water on the lower poorly drained sites every year during the rainy season, while adjacent sites may be well drained (Rosseti et al., 2005). This probably happens because interfluvial areas are lowland plains (Sombroek, 2000). In addition, the fluctuations of the underground water may generate a firm layer of varying depth by deposition of iron and other nutrients (Quesada et al., 2010), generating a complex hydrology that may influence ecosystem processes in ways much different both from the terra firme forests and the large rivers floodplain forests. The complex effects of soil, climate and hydrology on productivity of seasonally waterlogged interfluvial wetland forests are still poorly understood.

It must be considered that the Amazon basin will undergo a severe transition towards a disturbance-dominated regime, mostly due to changes in land-use and climate (Malhi et al., 2008; Cook et al., 2012; Davidson et al., 2012). Hence, the severe impacts caused by continuous deforestation and degradation in the Amazon Basin, mainly associated with the large infrastructural program of the Brazilian Federal Government, generate demands for rapid assessment of information to generate databases that help discriminate areas for forest management and conservation, and therefore contribute for a sustainable development of the Amazon region. In this context, information on tree growth, tree ages and forest productivity are important key data to establish criteria to define areas of conservation priorities and sustainable policies for sustainable management.

The most common field method to estimate wood productivity in the tropics is monitoring tree growth. However, only after many years of repeated diameter measurements in permanent plots, the estimates of diameter increment rates are reliable (Clark et al., 2001). Alternatively to monitoring tree growth, tree-ring analysis has been applied for reliable estimates of tree ages and mean diameter growth rates which are necessary to predict the woody biomass production. Recently, tree-ring data have successfully been used to estimate wood biomass productivity in different forest types of Central Amazonia (Stadtler, 2007; Oliveira, 2010; Schöngart et al., 2010) and also in the Pantanal wetlands (Schöngart et al., 2011). In the Amazon, annual tree rings occur in the non-flooded terra firme forests as a consequence of the rainfall seasonality with one dry and one rainy season during a year (Vetter, 1995; Worbes, 1989, 1999; Dünisch et al., 2003; Brienen and Zuidema, 2005; Zuidema et al., 2012). The rainfall seasonality in large catchment areas of the Amazon River and its large tributaries results in a monomodal flood-pulse also leading to the formation of annual tree ring in the wood of tree species in the floodplain forests (Worbes, 1989; Schöngart et al., 2002, 2004, 2005).

The presented study is the first field-based estimates for tree ages and wood biomass productivity in the vast interfluvial region between the Purus and Madeira rivers. We estimate aboveground wood biomass productivity in eight 1 ha plots distributed over 600 km along the interfluvial region between the Purus and Madeira Rivers. First, we assess wood biomass stocks by diameter, tree height and wood density applying two allometric models. Second, we use tree-ring data to estimate stand age and to model changes in biomass stocks over time. We than relate productivity and stand age to soil and hydrology conditions of the studied sites. Finally, we compare our results with other data of wood biomass productivity from different forest types of the Amazon basin and discuss their application in the context of conservation and forest management.

2 Material and methods

2.1 Study region

The study was carried out in the interfluvial area of the Purus-Madeira Rivers in the Amazonas State, Brazil, that is intersected by the BR-319highway connecting the cities of Manaus and Porto Velho, the capitals of the Amazonas and Rondonia states, respectively (Fig. 1).The dominant vegetation type in the northern part of this region is dense lowland rainforests, while in the south a transition towards open lowland rainforests occurs, probably caused by increasing rainfall seasonality (IBGE, 1997). The predominant soil type for the whole interfluvial region is Plinthosol/Gleysol (Martins et al., 2012). These soils have a firm plinthite layer that can change to hardpan if exposed to repeated wet and drying cycles (Quesada et al., 2011). On a local scale, frequent variations in the topography of a few meters create temporary pools on the lower and poorly drained areas during the rainy season (Rosetti et al., 2005). The duration and intensity of the rainy season varies strongly from north to south along the interfluvial area declining from 2800 to 2100 mm annual precipitation with increasing rainfall seasonality (ANA, 2011; Table 1).

As indicated by future scenarios the interfluvial region between the Madeira and Purus rivers will suffer huge impacts as a consequence of paving the BR-319 highway and the human occupation following in the next decades (Laurance et al., 2001; Soares-Filho et al., 2006; Fearnside et al., 2009; Davidson et al., 2012). To avoid deforestation, several conservation units (Sustainable Development Reserves, Extractive Reserves and State Forests) have been established along the highway. However, long-term scientific data on floristic composition, forest structure and dynamic are essential as a decision tool for the sustainable development of the region, as criteria for discrimination between areas of strict conservation or management priorities. In this context, a set of 11 research modules of the PRONEX project "Rapid Assessment for Long Duration Ecological Projects" (RAPELD) was established along the Purus-Madeira interfluvial region as part of the research modules network of the Research Program in Biodiversity (PPBio, http://ppbio.inpa.gov.br/sitios/br319).

2.2 Sampling design

In each of the 11 modules established along the interfluvial region of the Purus-Madeira rivers, ten 1 ha plots (250 × 40 m) were installed at every kilometer on two 5 km-long trails (Magnusson et al., 2005), totalizing 110 plots in the interfluvial region. Each plot followed an isocline to minimize variation in the topography and soil conditions within a plot (Magnusson et al., 2005). For this study, we selected four of the 11 modules (Table 1). The average distance between the modules was 140–200 km, spanning approximately 600 km distance (Fig. 1). At each area, we selected two of the 10 permanent plots, one on the highest altitude (well drained) and the other plot on the lowest topography (poorly drained),using SRTM-DEM data (Shuttle Radar Thematic Mapper Digital Elevation Model) (USGS, 2000; Farr et al., 2007).

2.3 Soil data

Soil samples were obtained every 50 m along the central 250 m long transect in all plots, totalizing six samples per plot. Soil samples of 30 cm depth were extracted with a borer and labeled and kept in sealed plastic bags for 2–5 days. On arrival at the laboratory, the samples were air dried at ambient temperature. After drying, composite samples were prepared from all points, resulting in one sample per plot. Soil texture was then analyzed following standard protocol of total dispersion using sodium pyrophosphate to obtain clay, sand and silt percentages (EMBRAPA, 2011). The soil phosphorus concentration was also analyzed, following protocol by EMBRAPA (2011). To analyze soil water saturation pits of 2 m depth were dug in modules M01, M05 and M08. To increase spatial coverage of soil water saturation scores corer samplings in each plot were used. Soil water saturation in each plot was scored using the classification index of Quesada et al. (2010) (Table 2), using soil samples up to 7 m depth collected by the HIDROVEG project and 2 m depth pit descriptions dug in modules M01, M05 and M08. Soil water saturation conditions classified by an index are based on the effective depth of the soil, hydrological properties and the presence of a plinthite layer, pointing to soil hydromorphic features. This index may be an important edaphic parameter as it appears to be related to vegetation parameters (Martins et al., 2012). All soil samples were collected in cooperation with the HIDROVEG project and analyzed at the Thematic Soils Laboratory of the National Institute for Amazon Research (INPA).

2.4 Topographical and hydrological conditions

Terrain hydrological conditions were assessed by using remote sensing and field data. The plots were preselected based on SRTM data to capture a wide range of topographies within and between the selected modules. Afterwards we applied the HAND model (height above the nearest drainage) that indicated the vertical distance of the plot from the nearest water-table as an indicator for the hydrological conditions (Rennó et al., 2008). The HAND value, based on SRTM data, was calculated for all plots (Moulatlet, 2010). We also used the soil water saturation index (Table 2) as a reliable indicator for the terrain's hydrological condition, to relate wood biomass productivity to soil hydrology. The difference between this index and the HAND value is that the HAND data describe hydrology based on topography, and therefore will be most effective in terrains with pronounced topographical variations, since the level of the groundwater table may vary with the elevation depending on the soil conditions. The water saturation index, on the other hand, is based on soil features that were developed by long-term underground water fluctuations, such as the depth of the plinthite layer (see Quesada et al., 2010), and is therefore a more reliable indicator for variations in soil water saturation of the study sites. HAND data can be obtained with less effort than the soil water saturation index, however, they are less reliable in terrains with a smooth topography as it is the case in our study region.

2.5 Field measurements

The RAPELD program records all trees with diameter at breast height (DBH) above 30 cm in the installed 1 ha plots. Trees with a DBH of 10–30 cm are considered on two 10 m large sections on both sides of the 250 m long transect in the middle of the plot (0.5 ha) (Magnusson et al., 2005). In this study, we considered all trees with DBH > 30 cm of the forest inventory (Schietti et al., unpublished data) in order to obtain data on wood densities as well as to estimate ages and diameter increment rates for each tree by growth-ring analysis. A total of 554 trees were sampled in the eight plots, from which 22 individuals were not considered due to very low distinction of the growth rings. Table 3 shows the number of sampled trees with DBH > 30 cm in each plot. The sampling effort per plot was 47 to 87 trees with DBH > 30 cm per hectare, corresponding to 53–96 % of all individuals of this diameter class. Further we sampled 30 randomly selected trees within the DBH classes 10–30 cm in each plot. Palm trees (Arecaceae) were not considered in this study.

The DBH of all trees was measured by a diameter tape. In case of buttresses, diameter was measured above them to avoid overestimates of basal area and wood biomass. Tree height was estimated using a height measurement device (Blume Leiss BL6). Two wood samples were extracted from the trunk of each tree using an increment borer of 5.15 mm internal diameter. The sampling of wood samples was made 10 cm below the DBH (120 cm above the forest floor) to avoid errors for future repeated diameter measurements with the aim to monitor forest dynamics. One sample was extracted for wood density determination. To avoid dehydration these samples were labeled with the plot and tree number and stored in closed plastic bags. The second sample was extracted to estimate radial increment rates. These wood samples were glued on wooden supports with identity numbers for plot and tree. All wood samples were transported to the Dendroecological Laboratory of the scientific cooperation between INPA and MPIC (Max Planck Institute for Chemistry) in Manaus for further analyses.

2.6 Botanical data

All sampled individuals are currently being identified by Priscila Souza and Carolina Levis. The botanical material was pre-identified in field with the help of a parataxonomist. After a preliminary identification, the botanical identification was confirmed with the aid of specialists, identification guides and by comparing the vouchers collected to specimens at the INPA Herbarium (Manaus, Brazil) and virtual herbariums (http://sciweb.nybg.org/science2/vii2.asp). Fertile specimens will be deposited at INPA and sterile material will be stored in an adjacent working collection. Plants were identified in accordance with the APGIII (Angiosperm Philogenetic Group III) classifications. For name correction of the taxa the Brazilian Flora Species List was consulted (http://floradobrasil.jbrj.gov.br/2012/).

2.7 Biomass and carbon stocks estimates

Information on the total basal area per hectare for the diameter classes 10–30 cm and above 30 cm was obtained from forest inventory data (J. Schietti et al., unpublished data). Since trees with DBH of 10–30 cm are sampled only on 0.5 ha in the existing inventory, information on basal area for this cohort was multiplied by factor two to obtain estimates for the entire hectare.

To calculate wood density (ρ) the fresh volume (V_{fresh}) of each sample was determined by the water displacement method. The wood sample was mounted on a needle and immersed into a recipient filled with water on an analytic balance calibrated to zero. The sample volume is equal to the indicated weight of the displaced water after submerging the sample entirely into the water without touching the side or the bottom of the recipient. After this step of analysis the samples were dried at a temperature of 105 °C to obtain their dry weight (W_{dry}) (Chave et al., 2005; Schöngart et al., 2005). Wood specific density was than calculated as:

$$\rho = \frac{W_{\text{dry}}}{V_{\text{fresh}}} \tag{1}$$

For each plot we calculated the mean wood density and standard deviation.

Since there are large distances between the four studied modules and the vegetation type shifts from the north to the south within the interfluvial region, possible differences in tree height and wood density between the areas can be expected (Chave et al., 2005; Wittmann et al., 2006; Nogueira et al., 2008a, b; Feldpausch et al., 2011). As there are no specific allometric models available for the studied forest types, two models from other biogeographic regions were used for estimates of aboveground wood biomass (AGWB) (Cannell, 1984; Chave et al., 2005).These models use diameter, height and wood density as independent parameters to enhance the quality of the

AGWB estimates (Chave et al., 2004, 2005; Schöngart et al., 2010, 2011) since the use of allometric equations with less than three independent parameters would lead to strong biases in the data (Feldpausch et al., 2012). For all of the equations described below, the parameters are referred as: aboveground coarse wood biomass (AGWB in kg), diameter at breast height (DBH in cm), tree height (H in m), and wood density (ρ in g cm^{-3}). Cannell (1984) used a constant form factor ($F = 0.06$) to estimate woody biomass for tree species from the pantropics as the following product:

$$\mathrm{AGWB}_1 = \pi \cdot \left(\frac{\mathrm{DBH}}{2}\right)^2 \cdot H \cdot \rho \cdot F \tag{2}$$

Chave et al. (2005) developed different allometric models for forests types submitted to different climate conditions. For lowland rainfall forests with a marked dry season of 1–4 months and 1500–3500 mm yr^{-1} rainfall, the following equation was developed:

$$\mathrm{AGWB}_2 = 0.0509 \cdot \mathrm{DBH}^2 \cdot H \cdot \rho \tag{3}$$

As not all trees of the plot were sampled we estimate the AGWB in relation to the basal area of the sampled trees. This was performed separately for the two diameter classes DBH > 30 cm (> 30) and trees with DBH 10–30 cm (< 30). Table 3 indicates the number and percentage of all sampled trees, trees which were sampled for additional wood density determinations and not sampled trees. For this study we assume that the carbon content ($C_{(\%)}$) of the AGWB depends on wood density (Elias and Potvin, 2003) estimated by:

$$C_{(\%)} = (\rho + 16.21)/0.3732 \tag{4}$$

To account for possible measurement errors in the field we performed an error propagation for our AGWB estimates. Errors in measurements of DBH were assumed as 1 %, 10 % for tree height and the standard deviation of the wood density of the plot for wood density (Schöngart et al., 2011). For allometric models (4) and (5), error propagations for the biomass estimates were calculated as in Schöngart et al. (2011):

$$\sigma \mathrm{AGWB}_1 = \left(\frac{\pi}{4}\right)^2 \cdot \left[\left(\sigma_F \cdot \mathrm{DBH}^2 \cdot H \cdot \rho\right)^2 + (\sigma_{\mathrm{DBH}} \cdot F \cdot 2\mathrm{DBH} \cdot H \cdot \rho)^2 + \left(\sigma_H \cdot F \cdot \mathrm{DBH}^2 \cdot \rho\right)^2 + \left(\sigma_\rho \cdot F \cdot \mathrm{DBH}^2 \cdot H\right)^2\right] \tag{5}$$

and

$$\sigma \mathrm{AGWB}_1 = \left[\left(0.00509 \cdot \mathrm{DBH}^2 \cdot H \cdot \rho\right)^2 + (\sigma_{\mathrm{DBH}} \cdot 0.0509 \cdot 2\mathrm{DBH} \cdot H \cdot \rho)^2 + \left(\sigma_H \cdot 0.0509 \cdot \mathrm{DBH}^2 \cdot \rho\right)^2 + \left(\sigma_\rho \cdot 0.0509 \cdot \mathrm{DBH}^2 \cdot H\right)^2\right] \tag{6}$$

2.8 Tree ring analysis and growth modeling

The prepared wood samples for tree-ring analysis were sanded and polished to produce a plain surface that enabled the visualization of the annual rings based on the wood anatomical analysis. Wood anatomy of tree rings was characterized following Worbes (2002): (1) intraannual variations of wood density within a tree ring where wood density increases from earlywood to latewood, typical for the families Annonaceae, Myrtaceae and Lauraceae; (2) tree rings delimited by marginal parenchyma bands commonly observed for species from the families Fabaceae, Meliaceae and Bignoniaceae; (3) alternated bands of parenchyma and fiber tissue, usually with higher fiber content at the beginning of the tree ring and higher parenchyma contents at the growth boundary commonly observed for the families Sapotaceae, Lecythidaceae, Combretaceae and Moraceae, and (4) ring-porous tree rings with larger vessels in the earlywood and smaller vessels in the latewood, rarely observed in the humid tropics (Fig. 2).

Ring widths were measured by a digital measuring device (LINTAB) with 0.01 mm precision attached to a computer with the software Time Series Analysis and Presentation (TSAP-WIN) to determine mean radial increments (Schöngart et al., 2004). On samples which contained the pith tree age was estimated by direct ring count. For samples with missing pith we estimated tree age by dividing the obtained average diameter increment rates by the measured DBH in the field. The mean tree age per plot was calculated as the average of the ages from all sampled trees with DBH > 30 cm ($\mathrm{Age}_{>30}$) and with DBH of 10–30 cm ($\mathrm{Age}_{<30}$), weighted by their basal areas ($\mathrm{BA}_{>30}$ and $\mathrm{BA}_{<30}$) in the plot:

$$\mathrm{AGE}_{\mathrm{PLOT}} = \frac{\left(\mathrm{AGE}_{>30} \cdot \mathrm{BA}_{>30}\right) + \left(\mathrm{AGE}_{<30} \cdot \mathrm{BA}_{<30}\right)}{\mathrm{BA}_{>30} + \mathrm{BA}_{<30}} \tag{7}$$

Non-linear regressions were carried out between DBH and tree height using potential equations to produce DBH-height relationships for each plot and module. The relationship between tree age and DBH was fitted to non-linear regression models (Schöngart, 2008):

$$\mathrm{AGE} = a \cdot e^{-b \cdot \mathrm{DBH}} \tag{8}$$

Estimation of forest productivity and carbon sequestration To estimate the AGWB productivity the cumulative diameter growth curve of a tree was combined with the stand-specific DBH-height regression model. Together with the information of wood density it is then possible to predict for every age along the entire life span the AGWB by the allometric models of Eqs. (2) and (3) (Schöngart et al., 2011). With these models we estimated the age-related aboveground wood biomass production of each tree ($\mathrm{AGWBP}_{\mathrm{tree}}$) calculating the average of the difference between the AGWB of consecutive years (t) (Eq. 9).

$$\mathrm{AGWBP}_{\mathrm{tree}} = \sum\nolimits_i^t \left(\mathrm{AGWB}_{i,\,t} - \mathrm{AGWB}_{i,\,t-1}\right)/t \tag{9}$$

Stand productivity was then calculated in two different ways, one to indicate the current total productivity of the stand and the other for data analysis to account for the long-term influence of environmental conditions on tree growth and wood biomass increments.

To indicate the current total productivity of the plot ($AGWBP_c$), $AGWBP_{tree}$ was calculated considering the last five growth rings of each tree (Eq. 9, $t = 5$). As not all trees of the plot were sampled we estimated the productivity in relation to the basal area for all sampled trees. This was performed separately for the two diameter classes DBH > 30 cm (> 30) and trees with DBH 10–30 cm (< 30) (Eq. 10). Relating the AGWB productivity per m^2 basal area multiplied by the total basal area in each diameter class gives an estimate of the stand's AGWB production. To account for the long-term influence of environmental conditions on tree growth and wood biomass increment ($AGWBP_m$), $AGWBP_{tree}$ was calculated considering the whole life span of each tree (Eq. 9). For data analysis, $AGWBP_m$ was calculated by Eq. 11 considering the mean value of both allometric equations. Then, in Eq. (11) $AGWBP_m$ was also divided by the stand's basal area (SCF – structural conversion factor; Malhi et al., 2006) to account for high structural differences between the plots:

$$AGWBP_c = \left(AGWB_{>30} \cdot \frac{BA_{Total}}{BA_{>30}} + AGWB_{<30} \cdot \frac{BA_{Total}}{BA_{<30}} \right), \quad (10)$$

$$AGWBP_{Mean} = \frac{\left(AGWB_{>30} \cdot \frac{BA_{Total}}{BA_{>30}} + AGWB_{<30} \cdot \frac{BA_{Total}}{BA_{<30}} \right)}{BA_{Total}} \quad (11)$$

Data analysis were carried out using R-statistics. Graphs were built using R-statistics.

3 Results

Table 4 shows basal area, mean canopy height, mean wood density, mean tree age and the non-linear regression models between DBH and tree height for each site. Tree height was measured for a total of 630 trees. In all four modules DBH explains 56–62 % of the variability in tree height, with exception of module M08 where the multiple R-squared is only 0.30 (Table 4).

Of all sampled trees one has 214 rings including the pith. Another has 239 rings without reaching the pith, resulting in an estimation of more than 500 yr by extrapolating the number of counted rings in relation to the mean radius of the tree trunk. By this calculation, we estimate that from all the sampled trees, 33 would be more than 200 yr old. The non-linear relationship between DBH and tree age from all plots is significant ($n = 534$, df = 532, $F = 108.65$, $R^2 = 0.29$, $p < 0.01$) (Fig. 3a). Only about 30 % of the variability of tree age among different species and varying growth condition can be explained by DBH, due to differences in growth rates between species and individuals of the same species growing in different environmental conditions. However, the strength of correlation is not sufficient to consider the model to estimate tree ages in the field only by measuring DBH, independent of the species. Table 5 indicates mean wood densities and radial increment rates for the most common species. Among the most abundant tree species wood density varies between 0.44± 0.11 g cm^{-3} (*Apeiba echinata*) and 0.90 ± 0.05 g cm^{-3} (*Licania oblongifolia*). The lowest mean annual radial increments are observed for *Pseudolmedia laevis* (1.1 ± 0.2 mm) and *Eschweilera coriacea* (1.1± 0.4 mm), while *A. echinata* presents radial increment rates of 3.4± 2.4 mm. On the stand level mean wood density is significantly related to the mean radial increments (n = 8, df = 7, $F = 11.12$, $R^2 = 0.65$, $p = 0.015$) (Fig. 3b).

Estimates of AGWB resulted in 233 Mg ha^{-1} with a standard deviation of 66 Mg ha^{-1} for the whole study region (Table 6). In relation to the basal area of the stand the AGWB stocks varies 7.6–12.1 Mg m$^{-2}_{\text{basal area}}$ (Eq. 3) and 8.2–13.1 Mg m$^{-2}_{\text{basal area}}$ (Eq. 4). The AGWBP varies between 3.3-3.9 Mg ha^{-1} yr^{-1} (Eq. 2) and 3.5–4.2 Mg ha^{-1} yr^{-1} (Eq. 3) in the seasonally flooded forests of module M01. For other plots productivity is much higher ranging between 5.5–6.4 Mg ha^{-1} yr^{-1} (Eq. 2) and 6.1–7.1 Mg ha^{-1} yr^{-1} (Eq. 3). The estimated C-sequestration ranges between 1.4–1.7 Mg C ha^{-1} yr^{-1} (Eq. 2) and 1.6–1.9 Mg C ha^{-1} yr^{-1} (Eq. 3) in the two seasonally flooded plots and between

2.4–2.9 $\text{Mg ha}^{-1}\,\text{yr}^{-1}$ (Eq. 2) and 2.7–3.2 $\text{Mg ha}^{-1}\,\text{yr}^{-1}$ (Eq. 3) in the other plots (Table 6). Our estimations of total AGWBP_C result in much lower values for the M01 seasonally floodplain plots compared to the plots of other modules. The estimates of AGWB and AGWBP produced by Eqs. (2) and (3) indicate only small differences.

AGWBP is here hypothesized to vary with soil structure and hydrology. A strong relation is presented between AGWBP_m (calculated from the average of all rings of a tree) and the soil water saturation index (Fig. 4a, $n = 8$, df = 6, $R^2 = 0.83$, $F = 30.44$, $p < 0.01$) representing the soil structure (effective depth) and hydrology. The soil water saturation index significantly affects the mean biomass production of the trees, once that increasing values of the index enhance AGWBP_m (Fig. 4a) and decreases plot's mean age ($n = 8$, df = 6, $R^2 = 0.7$, $F = 13.98$, $p < 0.01$) (Fig. 4b). This pattern is not observed when we related the biomass production of the trees to the HAND data ($n = 8$, df = 6, $R^2 = 0.04$, $F = 0.25$, $p > 0.05$). However, when the two seasonally flooded plots of M01 are removed from the analysis, we observed a relatively strong relation between biomass production of trees and the HAND data, close to significance ($n = 6$, df = 4, $R^2 = 0.61$, $F = 6.3$, $p = 0.06$), following the same pattern as observed with the water saturation index. Table 7 summarizes the soil data obtained for each plot. The soil texture of all plots is mainly composed by silt, with varying small percentages of sand and clay. The concentration of iron molecules, which is the main element associated with the formation of plinth soils, ranges considerably among the plots between 66.7 and 388.8 $\text{mg g}_\text{soil}^{-1}$. We find no correlation between productivity or stand age and any soil chemical property. However, since flooding on the M01 module is influenced by large river waters, soil chemical properties at M01 do not follow the same patterns as in other modules. Therefore, excluding the M01 plots, we noticed a very strong correlation between total productivity and available phosphorus in the soil ($n = 6$, df = 4, $R^2 = 0.76$, $F = 13.21$, $p < 0.01$) (Fig. 5a). We find no relation between the water saturation index and the phosphorus concentration in our plots, but on a regional scale, there is a positive correlation between the concentration of available phosphorus and the water saturation index ($n = 42$, df = 40, $R^2 = 0.16$, $F = 7.76$, $p < 0.01$) (Fig. 5b).

Title Page
Abstract | Introduction
Conclusions | References
Tables | Figures
◀| |▶
◀ ▶
Back | Close
Full Screen / Esc
Printer-friendly Version
Interactive Discussion

4 Discussion

The presented data on tree ages, diameter growth, estimates on AGWB and forest productivity indicate old-growth forests with large stocks of AGWB and relatively high AGWBP, at the range of the nutrient-rich várzea floodplains (Nebel et al., 2001; Schöngart et al., 2010) and paleovárzeas (Stadtler, 2007) (Table 6), despite the low soil fertility of the area (RADAMBRASIL, 1978). However, the AGWBP of the studied forests varies considerably between 3.4–6.8 Mg ha^{-1} yr^{-1} (Table 5).

We find increasing wood biomass productivity with increasing water-logging indicated by the soil water saturation index. This is surprising, since flooding or water-saturated soils cause anoxic conditions (Lambers et al., 2007; Kursar et al., 2008; Haase and Rätsch, 2010; Piedade et al., 2010), leading to a decrease in diameter growth (Schöngart et al., 2002) and a decline in forest productivity, as Stadtler (2007) indicated for the nutrient-poor black-water floodplain forests along a hydrological gradient in the Amanã Sustainable Development Reserve, Amazonas state, Brazil. However, the surveillance of tree growth in floodplain forests reveal that trees start growing within the dry season, when forests are still flooded (Schöngart et al., 2002). That could indicate that the conditions of saturation and flooding may generate different responses of tree growth, with water saturation being favorable for tree growth while flooding being unfavorable for tree growth.

The increase in the wood biomass productivity is not observed when using HAND data. However, not considering the two seasonally flooded plots in the analysis, the HAND data reveals a negative correlation with the total ABWBP in accordance with the results obtained using the soil water saturation index. Those two referred plots, despite being seasonally flooded, are scored with a lower soil saturation index than another plot that is saturated but not flooded. Therefore, the structure of the soil related to hydrology (i.e. soil depth, drainage and duration of the saturation period) seems to be more important for the productivity of trees than just the water level described by the HAND data and height of the water column. Indeed, during field work it became apparent that the HAND data does not describe well the local hydrology related to the smooth topography of the terrain and the inundation of the seasonally flooded plots, and thus is not a reliable data base to relate hydrology with estimated forest productivity alone.

Soil water saturation may vary with soil type and topography of the area. As described by Quesada et al. (2010, 2011) plinthosols, which are quite common in the study region, develop under non-optimal soil conditions by deposition of nutrients like iron. The phosphorus in these soils remains mainly associated with iron and is liberated when the oxidized iron is reduced in the flooded plinthite layer (Chacon et al., 2006). Under these conditions it is thinkable that hydromorphic soil characteristics influence the phosphorus availability in the soil, which in addition with the poor soil structure presented on each area, affects wood productivity of the different stands. This hypothesis is corroborated by the observed correlations between total wood biomass productivity and available phosphorus as well as between the regional variation of available phosphorus and the water saturation index. On the most saturated areas with poor soil structure, more plant-available phosphorus can be found. In the generally nutrient-poor soils of the study region (RADAMBRASIL, 1978) the release or reduction of one growth-limiting nutrient could possibly be sufficient to have strong impacts on forest growth. On well-drained soils, there is less reduction of the oxidized iron and as a consequence phosphorus would become more and more unavailable for the roots due to the strong fixation by the present oxidized iron, leading to reduced tree growth. A similar pattern was indicated by Clawson et al. (2001) at a semi-deciduous forest in the SW-USA indicating an increase in forest productivity with decreasing soil drainage, where phosphorus releasing was associated to reduction of oxidized iron in bad drained soils.

The variations in wood biomass productivity cannot, however, be associated with the chemical reactions of the soil alone. We show that there is indeed a variation of available phosphorus with the water saturation index, but that variation is still weak. We think the physical constrains related to the bad hydromorphic structure of the soil is also a very strong factor. It is possible that the water-logging of the soils at different depths of the plinthite layer acts as an environmental filter, creating a trade-off where plants would grow faster and present shorter life-cycles. This hypothesis is supported by the strong trend we found between the soil water saturation index and stand age. A high productivity means that trees grow faster and achieve larger diameters at lower ages. Water-logging can lead to shifts in species compositions as it is well known form Amazonian floodplain forests (Wittmann et al., 2006, 2010) towards tree species with higher growth rates and shorter life cycles. In this case we would expect a lower wood density for those tree species compared to slow-growing tree species (Gourlet-Fleury et al., 2011) that attain high ages, which is not the case for our studied forests. Still, despite the low variation of mean wood density, we find a significant negative relationship between mean radial increments and wood density between the studied sites which suggests that there is possibly a shift in tree species composition. Such variation could be a consequence of water-logging in the soils, leading to species assemblies with faster growth rates and shorter life spans due to special adaptations as it is described for trees in the central Amazonian floodplains (Parolin et al., 2004).

A third explanation could be that during the dry season water-logged sites provide a better water supply for tree growth than well-drained sites where tree growth is reduced during the dry season (Brienen and Zuidema, 2005). In this case we would expect varying climate-growth relationships between well and poorly drained soils. This is a hypothesis to be tested in future studies applying dendroclimatology for characteristic tree species from different ecotypes between well-drained and water-logged soils in the interfluvial region using traditional tree ring analysis and stable isotopes analyses. We predict that the vegetation period of tree species varies temporarily between different forest types depending on the soil type and hydrological regime such as it was observed between floodplain forests and adjacent terra firme forests in Central Amazonia (Schöngart et al., 2004, 2010).

In Table 8 we compare the results for AGWB and AGWBP in this study with other studies in different regions of the Amazon basin. The AGWB stocks in the studied forests of the interfluvial landscape of the Madeira-Purus region are lower than in terra firme forests, but higher than in floodplain forests and old fluvial terraces (paleovárzeas). Comparing the woody biomass productivity our studied forests indicate a similar AGWBP as paleovárzeas and várzeas. In comparison to the seasonally flooded and nutrient-poor igapó and the Central Amazonian terra firme forests the studied forest present a higher AGWBP. Only the Southwestern Amazonian terra firme forests seem to be more productive, however, as Malhi et al. (2004) applied allometric models which do not consider tree height for the estimates of AGWBP, the values could present biases in the estimates (Schöngart et al., 2010; Feldpausch et al., 2012).

We conclude that AGWBP in the study region is as high as in várzea and paleovárzea regions that are among the most productive forest types in the Amazon basin. Productivity varies with the hydrological conditions, but it seems that variation in the soil water saturation has even a bigger impact on forest productivity then simply the topographic variation of the terrain. However, it remains unclear to us whether hydrological, climatic or edaphic properties or a combination of all control productivity of these forests, since the structure of soils in the area is strongly determined by underground water fluctuations.

A high natural productivity of a forest ecosystem is one of the criteria for the development of sustainable forest management plans (Schöngart and Queiroz, 2010). However, the extraction of timber resources in tropical forests as practiced in general is not sustainable (Brienen and Zuidema, 2006, 2007; Schöngart, 2008; Shearman et al., 2012). In our study region, the most productive sites are encountered on poorly structured soils. The poor structure will probably lead to slow recover of the forest after extracting, and therefore make extraction of timber resources not sustainable. Species and site specific forest managements have to be developed as it was formulated by the GOL-concept (Growth-Oriented Logging) for the high-productive várzea floodplain forests of Central Amazonia (Rosa, 2008; Schöngart, 2008, 2010), that resulted in the Normative Instruction (IN)no. 009. In this forest legislation timber resource management was differentiated for fast-growing tree species with low wood densities (madeira branca) and those with high wood densities above 0.60 g cm^{-3} (madeira pesada),

Title Page
Abstract Introduction
Conclusions References
Tables Figures
◀◀ ▶▶
◀ ▶
Back Close
Full Screen / Esc
Printer-friendly Version
Interactive Discussion

applying felling-cycles of 12 and 24 yr, respectively, and species-specific minimum logging diameters. Species-specific and site-specific growth models based on tree rings together with studies on the regeneration dynamics and population structure should be performed to evaluate the potential of forest management plans for the region where huge complexes of conservation units have been established allowing the sustainable use of timber resources.

General global climate models predict a huge impact for the Amazon basin and its carbon stocks and uptakes, mainly due to shifts in the precipitation and hydrological regimes (Dufresne et al., 2002; Betts et al., 2004; Cook et al., 2012). These changes are mainly caused by the increase of sea surface temperature (SST) anomalies in the Equatorial Pacific (Sombroek, 2001; Foley et al., 2002; Marengo, 2004; Schöngart and Junk, 2007) and the tropical Atlantic Oceans (Tomasella et al., 2010; Yoon and Zeng, 2010). During the severe drought events in 2005 and 2010, which affected between 2.5 and 3.2 million square kilometers in the Amazon basin, respectively, the interfluvial region between Purus and Madeira Rivers suffered negative precipitation anomalies in 2005 and 2010 (Phillips et al., 2009; Lewis et al., 2011). However, it is unknown how such severe droughts affect the patchwork of floodplain forests, forests on waterlogged soils and well-drained site. Tree species in Amazonia within the same stand and between ecosystems present varying climate-growth relationships (Worbes, 1999; Schöngart et al., 2002, 2004, 2010; Dünisch et al., 2003; Brienen and Zuidema, 2005) and may present varying responses to soil water saturation (Rodríguez-González et al., 2010). More field data are necessary to relate recruitment and mortality rates to interannual climate and hydrological variation. Such data are essential for the sustainable development of this particular region in terms of timber resource management and conservation as well as future scenarios for carbon stocks, emissions and uptakes due to changes in land-use and climate change.

Acknowledgements. We thank the Coordenação de Aperfeiçoamento de Pessoal de Nível Superior (CAPES) for financial support; the National Institute for Amazon Research – INPA, for providing all the infrastructure for the laboratories; the Project INPA/Max Planck for financing, providing laboratories and logistics; the PPBio/CENBAM for financing and providing all field infrastructure and the HIDROVEG project for logistics support for all fields expeditions in the BR-319.

The service charges for this open access publication
have been covered by the Max Planck Society.

References

Agência Nacional das Águas: http://hidroweb.ana.gov.br/, 28 February 2012.

Baker, T. R., Phillips, O. L., Malhi, Y., Almeida, S., Arroyo, L., Di Fiori, A., Erwin, T., Higuchi, N., Killeen, T. J., Laurance, S. G., Laurance, W. F., Lewis, S. L., Monteagudo, A., Neill, D. A., Vargas, P. N., Pitman, N. C. A., Silva, J. N. M., and Martínez, R. V.: Increasing biomass in Amazonian forest plots, Philos. T. Roy. Soc. B, 359, 353–365, 2004.

Betts, R. A., Cox, P. M., Collins, M., Harris, P. P., Huntingford, C., and Jones, C. D.: The role of ecosystem-atmosphere interactions in simulated Amazonian precipitation decrease and forest dieback under global climate warming, Theor. Appl. Climatol., 78, 157–155, 2004.

Brienen, R. J. W. and Zuidema, P. A.: Relating tree growth to rainfall in Bolivian rain forests: a test for six species using tree ring analysis, Oecologia, 146, 1–12, 2005.

Brienen, R. J. W. and Zuidema, P. A.: The use of tree rings in tropical Forest management: projecting timber yields of four Bolivian tree species, Forest Ecol. Manag., 226, 256–267, 2006.

Brienen, R. J. W. and Zuidema, P. A.: Incorporating persistent tree growth differences increases estimates of tropical timber yield, Front. Ecol. Environ., 5, 302–306, 2007.

Cannell, M. G. R.: Woody biomass of forest stands, Forest Ecol. Manag., 8, 299–312, 1984.

Chambers, J. Q., Santos, J., Ribeiro, R. J., and Higuchi, N.: Tree damage, allometric relationships, and above-ground net primary production in central Amazon forest, Forest Ecol. Manag., 152, 73–84. 2001.

Chave, J., Condit, R., Aguilar, R., Hernandez, A., Lao, L., and Perez, L.: Error propagation and scaling for tropical forest biomass estimates, Philos. T. Roy. Soc. B, 359, 409–420, 2004.

Chave, J., Andalo, C., Brown, S., Cairns, M. A., Chambers, J. Q., Eamus, D., Fölster, H., Fromard, F., Higuchi, N., Kira, T., Lescure, J. -P., Nelson, B. W., Ogawa, H., Puig, H., Riéra, B., and Yamakura, T.: Tree allometry and improved estimation of carbon stocks and balance in tropical forests, Oecologia, 145, 87–99, 2005.

Clark, D. A., Brown, S., Kicklighter, D. W., Chambers, J. Q., Thomlinson, J. R., Ni, J., and Holland, E. A.: Net primary production in tropical forest: an evaluation and synthesis of existing field data, Ecol. Appl., 11, 371–384, 2001.

Chacon, N., Silver, W. L., Dubinsky, E. A., and Cusack, D. F. Iron reduction and soil phosphorous solubilization in humid tropical forest soils: the roles of labile carbon pools and an electron shuttle compound, Biogeochemistry, 78, 67–84, 2006.

Clawson, R .G., Lockaby, B. G., and Rummer, B. Changes in Production and Nutrient Cycling across a Wetness Gradient within a Floodplain Forest, Ecosystems, 4, 126–138, 2001.

Cook, B., Zeng, N., and Yoon, J.-H.: will Amazonia Dry Out? Magnitude and Causes of Change from IPCC Climate Model Projections, Earth Interact., 16, 1–27, 2012.

Corlett, R. T.: Impact of warming on tropical lowland forests, Trends Ecol. Evol., 26, 606–613, 2011.

Davidson, E. A., Araújo, A. C., Artaxo, P., Balch, J. K., Brown, I. F., Bustamante, M. C. M., Coe, M. T., De Fries, R. S., Keller, M., Longo, M., Munger, J. W., Schroeder, W., Soares-Filho, B. S., Souza Jr., C. M., and Wofsy, S. C.: The Amazon basin in transition, Nature, 481, 321–328, 2012.

Dufresne, J. -L., Friedlingstein, P., Berthelot, M., Bopp, L., Ciais, P., Fairhead, L., Le Treut, H., and Monfray, P.: On the magnitude of positive feedback between future climate change and the carbon cycle, Geophys. Res. Lett., Geophys. Res. Lett., 29, 43-1–43-4, doi:10.1029/2001GL013777, 2002.

Dünisch, O., Montóia, V. R. M., and Bauch, J.: Dendroecologiacal investigations on *Swietenia macrophylla* King and *Cedrela odorata* L. (Meliaceae) in the central Amazon, Trees-Struct. Funct., 17, 244–250, 2003.

Elias, M. and Potvin, C.: Assessing inter- and intra-specific variation in trunk carbon concentration for 32 neotropical tree species, Can. J. Forest Res., 33, 1039–1045, 2003.

Donagema, G. K., Campos, D. V. B., Calderano, S., B., Teixeira, W. G., and Viana, J. H. M.: Manual de métodos de análise de solo, EMBRAPA SOLOS, Brazil, Rio de Janeiro, 2011.

Farr, T. G., Rosen, P. A., Caro, E., Crippen, R., Duren, R., Hensley, S., Kobrick, M., Paller, M., Rodriguez, E., Roth, L., Seal, D., Shaffer, S., Shimada, J., Umland, J., Werner, M., Oskin, M., Burbank, D., and Alsdorf, D.: The shuttle radar topography mission, Rev. Geophys., 45, RG2004, doi:10.1029/2005RG000183, 2007.

Fearnside, P. M., Graça, P. M. L. A., Keizer, E. W. H., Maldonado, F. D., Barbosa, R. I., and Nogueira, E. M.: Modelagem de desmatamento e emissões de gases de efeito estufa na BR-319, Revista Brasileira de Meteorologia, 24, 208–233, 2009.

Feldpausch, T. R., Banin, L., Phillips, O. L., Baker, T. R., Lewis, S. L., Quesada, C. A., Affum-Baffoe, K., Arets, E. J. M. M., Berry, N. J., Bird, M., Brondizio, E. S., de Camargo, P., Chave, J., Djagbletey, G., Domingues, T. F., Drescher, M., Fearnside, P. M., França, M. B., Fyllas, N. M., Lopez-Gonzalez, G., Hladik, A., Higuchi, N., Hunter, M. O., Iida, Y., Salim, K. A., Kassim, A. R., Keller, M., Kemp, J., King, D. A., Lovett, J. C., Marimon, B. S., Marimon-Junior, B. H., Lenza, E., Marshall, A. R., Metcalfe, D. J., Mitchard, E. T. A., Moran, E. F., Nelson, B. W., Nilus, R., Nogueira, E. M., Palace, M., Patiño, S., Peh, K. S.-H., Raventos, M. T., Reitsma, J. M., Saiz, G., Schrodt, F., Sonké, B., Taedoumg, H. E., Tan, S., White, L., Wöll, H., and Lloyd, J.: Height-diameter allometry of tropical forest trees, Biogeosciences, 8, 1081–1106, doi:10.5194/bg-8-1081-2011, 2011.

Feldpausch, T. R., Lloyd, J., Lewis, S. L., Brienen, R. J. W., Gloor, M., Monteagudo Mendoza, A., Lopez-Gonzalez, G., Banin, L., Abu Salim, K., Affum-Baffoe, K., Alexiades, M., Almeida, S., Amaral, I., Andrade, A., Aragão, L. E. O. C., Araujo Murakami, A., Arets, E. J. M. M., Arroyo, L., Aymard C., G. A., Baker, T. R., Bánki, O. S., Berry, N. J., Cardozo, N., Chave, J., Comiskey, J. A., Alvarez, E., de Oliveira, A., Di Fiore, A., Djagbletey, G., Domingues, T. F., Erwin, T. L., Fearnside, P. M., França, M. B., Freitas, M. A., Higuchi, N., E. Honorio C., Iida, Y., Jiménez, E., Kassim, A. R., Killeen, T. J., Laurance, W. F., Lovett, J. C., Malhi, Y., Marimon, B. S., Marimon-Junior, B. H., Lenza, E., Marshall, A. R., Mendoza, C., Metcalfe, D. J., Mitchard, E. T. A., Neill, D. A., Nelson, B. W., Nilus, R., Nogueira, E. M., Parada, A., Peh, K. S.-H., Pena Cruz, A., Peñuela, M. C., Pitman, N. C. A., Prieto, A., Quesada, C. A., Ramírez, F., Ramírez-Angulo, H., Reitsma, J. M., Rudas, A., Saiz, G., Salomão, R. P., Schwarz, M., Silva, N., Silva-Espejo, J. E., Silveira, M., Sonké, B., Stropp, J., Taedoumg, H. E., Tan, S., ter Steege, H., Terborgh, J., Torello-Raventos, M., van der Heijden, G. M. F., Vásquez, R., Vilanova, E., Vos, V. A., White, L., Willcock, S., Woell, H., and Phillips, O. L.: Tree height integrated into pantropical forest biomass estimates, Biogeosciences, 9, 3381–3403, doi:10.5194/bg-9-3381-2012, 2012

Flora do Brasil: Lista de Espécies da Flora do Brasil, http://floradobrasil.jbrj.gov.br/2012/, 11 December 2012.

Foley, J. A., Botta, A., Coe, M. T., and Costa, M. H.: El Niño-Southern Oscillation and the climate, ecosystems and rivers of Amazonia, Global Biogeochem. Cy., 16, 1132, doi:10.1029/2002GB001872, 2002.

Giardin, C. A. J., Malhi, Y., Aragão, L. E. O. C., Mamani, M., Huaraca Huaso, W., Durand, L., Feeley, K. J., Rapp, J., Silva-Espejo, E., Silman, M., Salinas, M., and Whittaker, R. J.: Net primary productivity allocation and cycling of carbon along a tropical forest elevational transect in the Peruvian Andes, Global Change Biol., 16, 3176–3192, 2010.

Gourlet-Fleury, S., Rossi, V., Rejou-Mechain, M., Freycon, V., Fayolle, A., Saint-André, L., Cornu, G., Gérard, J., Sarrailh, J. -M., Flores, O., Baya, F., Billand, A., Fauvet, N., Gally, M., Henry, M., Hubert, D., Pasquier, A., and Picard, N.: Envionmental filtering of dense-wooded species controls above-ground biomass stores in African Moist Forests, J. Ecol., 99, 981–990, 2011.

Haase, K. and Rätsch, G.: The morphology and anatomy of tree roots and their aeration strategies, in: Central Amazonian Floodplain Forests: Ecophysiology, Biodiversity and Sustainable Management, edited by: Junk, W. J., Piedade, M. T. F., Wittmann, F., Schöngart, J., and Parolin, P., Ecological Studies, 210, Springer Verlag, Dordrecht-Heidelberg-London-New York, 141–161, 2010.

IBGE: Recursos naturais e meio ambiente: uma visão do Brasil, Instituto Brasileiro de Geografia e Estatística, Brasil, 2nd Edn., 1997.

Instituto Nacional de Pesquisas da Amazônia (INPA), Manaus, Brazil: Programa de Pesquisa em Biosidersidade – PPBio, www.ppbio.inpa.gov.br, 20 February 2012.

Junk, W. J., Piedade, M. T. F., Schöngatr, J., Cohn-Haft, M., Adeney, J. M. and Wittmann, F.: A Classification of Major Naturally-Occurring Amazonian Lowland Wetlands, Wetlands, 31, 623–640, 2011.

Kursar, T. A., Wright, J., and Radulovivh, R.: The effects of the rainy season and irrigation on soil water and oxygen in a seasonal forest in Panama, J. Trop. Ecol., 11, 497–516, 1995.

Lambers, H., Chapin III, F. S. and Pons, T. L.: Plant Physiologycal Ecology. Springer Science + Business Media, USA, New York, 2nd Edn, 604 pp., 2007.

Laurance, W. F., Cochrane, M. A., Bergen, S., Fearnside, P. M., Delamônica, P., Barber, C., D'Angelo, S., and Fernandes, T.: The future of the Brazilian Amazon, Science, 291, 438–439, 2001.

Lewis, S. L., Brando, P., Phillips, O. L., van der Heijden, G. M. F., and Nepstad, D.: The 2010 Amazon Drought, Science, p. 331, 554, 2011.

Magnusson, W. E., Lima, A. P., Luizão, R., Luizão, F., Costa, F. R. C., Castilho, C. V., and Kinupp, V. R.: RAPELD: a modification of the Gentry method for biodiversity surveys in long-term ecological study sites, Biota Neotropica, 5, 1–6, 2005.

Malhi, Y., Baker, T. R., Phillips, O. L., Almeida, S., Alvarez, E., Arroyo, L., Chave, J., Czimczik, C. I., Di Fiori, A., Higuchi, N., Killeen, T. J., Laurance, S. G., Laurance, W. F., Lewis, S. L., Montoya, L. M. M., Monteagudo, A., Neill, D. A., Vargas, P. N., Patiño, S., Pitman, N. C. A., Quesada, C. A., Salomão, R., Silva, J. N. M., Lezama, A. T., Martínez, R. V., Terborgh, J., Vinceti, B., and Lloyd, J.: The above-ground coarse wood productivity of 104 Neotropical forest plots, Global Change Biol., 10, 563–591, 2004.

Malhi, Y., Wood, D., Baker, T. R., Wright, J., Phillips, O. L., Cochrane, T., Meir, P., Chave, J., Almeida, S., Arroyo, L., Higuchi, N., Killeen, T. J., Laurance, S. G., Laurance, W. F., Lewis, S. L., Monteagudo, A., Neill, D. A., Vargas, P. N., Pitman, N. C. A., Quesada, C. A., Salomão, R., Silva, J. N. M., Lezama, A. T., Terborgh, J., Martínez, R. V., and Vinceti, B.: The regional variation of aboveground live biomass in old-growth Amazonian forest, Global Change Biol., 12, 1–32, 2006.

Malhi, Y., Roberts, J. T., Betts, R. A., Killeen, J. T., Li, W., and Nobre, C. A.: Climate change, deforestation, and the fate of the Amazon, Science, 319, 169–172, 2008.

Marengo, R.: Interdecadal variability and trends of rainfall across the Amazon basin, Theor. App. Climatol., 78, 79–96, 2004.

Martins, D. L., Schietti, J., Luizão, F. J., Phillips, O., Andrade, A., Castilho, Andrade, A., C. V., Laurance, S.G., Oliveira, A., Toledo, J. J., Lugli, L.F. Mendoza, E.M.O., Feldpausch, T. R., and Quesada, C. A.: Soil induced changes on vegetation drive necromass stocks in Central Amazonia, Plant Ecology Diversity, special ed., in review, 2012.

Miranda, E. E. de (Coord): Brasil em Relevo, Campinas, Embrapa, Monitoramento por Satélite, 2005. Available in: Brasil em Relevo, Embrapa monitoramento por satélite, http://www.relevobr.cnpm.embrapa.br, 29 March 2013.

Moulatlet, G. M.: A importância de condições hidrológicas na distribuição e conservação de plantas herbáceas de sub-bosque em florestas amazônicas: uma contribuição em escala regional,M.Sc. Thesis, Brazil, National Institute for Amazon Research, 51 pp., 2010.

NASA Jet Propulsion Laboratory, California Institute of Technology: US Geological Survey, http://www.usgs.gov, 29 February 2012.

Nebel, G., Dragsted, J., and Salazar Vega, A.: Litter fall, biomass and net primary production in flood plain forests in the Peruvian Amazon, Forest Ecol. Manag., 150, 93–102, 2001.

Nogueira, E. M., Fearnside, M. P., Nelson, B. N., Barbosa, R. I., and Keizer, E. W. H.: Estimates of forest biomass in the Brazilian Amazon: new allometric equations and adjustments to biomass from wood-volume inventories, Forest Ecol. Manag., 256, 1853–1867, 2008a.

Nogueira, E. M., Nelson, B. W., Fearnside, P. M., França, M. B., and Oliveira, A. C. A.: Tree height in Brazil's arc of deforestation: shorter trees in south and southwest imply lower biomass, Forest Ecol. Manag., 255, 2963–2972, 2008b.

Oliveira, C. L.: Estimativas da dinâmica de carbono na biomassa lenhosa de terra firme na Reserva de Desenvolvimento Sustentável Amanã por métodos dendrcronológicos, M.Sc. thesis, National Institute for Amazon Research, 43 pp., 2010.

Parolin, P., Wittmann, F., Schöngart, J., and Piedade, M. T. F.: Amazonian várzea forests: adaptative strategies of trees as tools for forest management, Ecol. Appl., 3, 180–184, 2004.

Piedade, M. T. F., Ferreira, C. S., Oliveira Wittmann, A., Buckeride, M., and Parolin, P.: Biochemistry of Amazonian floodplain trees, in: Central Amazonian Floodplain Forests: Ecophysiology, Biodiversity and Sustainable Management, edited by: Junk, W. J., Piedade, M. T. F., Wittmann, F., Schöngart, J., and Parolin, P., Ecological Studies, 210, Springer Verlag, Dordrecht-Heidelberg-London-New York, 419–436, 2010.

Phillips, O. L., Aragão, L. E. O. C., Lewis, S. L., Fischer, J. B., Lloyd, J., López-Gonzales, G., Malhi, Y., Monteagudo, A., Peacock, J., Quesada, C. A., vam-der-Heijden, G., Almeida, S., Amaral, L., Arroyo, L., Aymard, G., Baker, T. R., Bánki, O., Blanc, L., Bonal, D., Brando, P., Chave, J., Oliveira, A. C. A., Cardozo, N. A., Czimczik, C. I., Feldpausch, T. R., Freitas, M. A., Gloor, E., Higushi, N., Jiménez, E., Lloyd, G., Meir, P., Mendoza, P., Morel, A., Neill, D. A., Nepstad, D., Patiño, S., Peñuela, M. C., Prieto, A., Ramírez, F., Schwartz, M., Silva, J., Silveira, M., Thomas, A. S., ter-Steege, H., Stropp, J., Vásquez, R., Zelazowski, P., Dávila, E. A., Andelman, S., Andrade, A., Chao, K. J., Erwin, T., Di-Fiore, A., Honório, E., Keeling, H., Kileen, T. J., Laurance, W. F., Cruz, A. P., Pitman, N. C. A., Vergas, P. N., Ramírez-Angulo, H., Rudas, A., Salamão, R., Silva, N., Terborgh, J., and Torres-Lezama, A.: Drought sensitivity of the Amazon forest, Science, 323, 1344–1347, 2009.

Quesada, C. A., Lloyd, J., Schwarz, M., Patiño, S., Baker, T. R., Czimczik, C., Fyllas, N. M., Martinelli, L., Nardoto, G. B., Schmerler, J., Santos, A. J. B., Hodnett, M. G., Herrera, R., Luizão, F. J., Arneth, A., Lloyd, G., Dezzeo, N., Hilke, I., Kuhlmann, I., Raessler, M., Brand, W. A., Geilmann, H., Moraes Filho, J. O., Carvalho, F. P., Araujo Filho, R. N., Chaves, J. E., Cruz Junior, O. F., Pimentel, T. P., and Paiva, R.: Variations in chemical and physical properties of Amazon forest soils in relation to their genesis, Biogeosciences, 7, 1515–1541, doi:10.5194/bg-7-1515-2010, 2010.

Quesada, C. A., Lloyd, J., Anderson, L. O., Fyllas, N. M., Schwarz, M., and Czimczik, C. I.: Soils of Amazonia with particular reference to the RAINFOR sites, Biogeosciences, 8, 1415–1440, doi:10.5194/bg-8-1415-2011, 2011.

RADAMBRASIL: Levantamento dos Recursos Naturais, Ministério de Minas e Energia, Departamento Nacional de Produção Mineral, Rio de Janeiro, Brazil, 1978.

Rennó, C. D., Nobre, A. D., Cuartas, L. A., Soares, J. V., Hodnett, M. G., Tomasella, J., and Waterloo, M. J.: HAND, a new terrain descriptor using SRTM-DEM: Mapping terra-firme rainforest environments in Amazônia, Remote Sens. Environ., 2008.

Rodríguez-González, P. M., Stella, J. C., Campello, F., Ferreira, M. T., and Albuquerque, A.: Subsidy or stress? Tree structure and growth in wetland forests along a hydrological gradient in Southern Europe, Forest Ecol. Manag., 259, 2015–2025, 2010.

Rosa, A. S.: Modelos de Crescimento de Quatro Espécies Madeireiras de Floresta de Várzea Alta da Amazônia Central por meio de Métodos Dendrocronológicos, MSc Thesis INPA/UFAM, Manaus, Brazil, 2008.

Rosetti, D. F., Toledo, P. M., and de-Góes, A. M.: New geological framework for Western Amazonia (Brazil) and implications for biogeography and evolution, Quaternary Res., 63, 78–89, 2005.

Saatchi, S. S., Houghton, R. A., dos Santos Avalá, R. C., Soares, J. V., and Yo, Y.: Distribution of aboveground live biomass in the Amazon basin, Global Change Biol., 13, 816–837, 2007.

Schöngart, J.: Growth Oriented Logging (GOL): A new concept towards sustainable forest management in Central Amazonian várzea floodplains, Forest Ecol. Manag., 256, 46–58, 2008.

Schöngart, J. and Junk, W. J.: Forecasting the flood-pulse in central Amazonia by ENSO-indices, J. Hydrol., 335, 124–132, 2007.

Schöngart, J. and Queiroz, H. L.: Timber extraction in the Central Amazonian floodplains, in: Central Amazonian Floodplain Forests: Ecophysiology, Biodiversity and Sustainable Management, edited by: Junk, W. J., Piedade, M. T. F., Wittmann, F., Schöngart, J., and Parolin, P., Ecological Studies, 210, Springer Verlag, Dordrecht-Heidelberg-London-New York, 419–436, 2010.

Schöngart, J., Piedade, M. T. F., Ludwigshausen, S., Horna, V., and Worbes, M.: Phenology and stem-growth periodicity of tree species in Amazonian floodplain forests, J. Trop. Ecol., 18, 581–597, 2002.

Schöngart, J., Junk, W. J., Piedade, M. T. F., Ayres, J. M., Hüttermann, A., and Worbes, M.: Teleconnection between tree growth in the Amazonian floodplains and the El Niño Southern Oscillation effect, Global Change Biol., 10, 683–692, 2004.

Schöngart, J., Piedade, M. T. F., Wittmann, F., Junk, W. J., and Worbes, M.: Wood growth patterns of *Macrolobium acaciifolium* (Benth.) Benth.(Fabaceae) in Amazonian black-water and white-water floodplain forests, Oecologia, 145, 454–461, 2005.

Schöngart, J., Wittmann, F., and Worbes, M.: Biomass and NPP of Central Amazonian floodplain forests, in: Amazonian floodplainforests: Ecophysiology, biodiversity and sustainable management, edited by: Junk, W. J., Piedade, M. T. F., Wittmann, F., Schöngart, J., and Parolin, P., Ecological Studies, Springer Verlag, Dordrecht, Heidelberg, London, New York, 347–388, 2010.

Schöngart, J., Arieira, J., Felfili Fortes, C., Cezarine de Arruda, E., and Nunes da Cunha, C.: Age-related and stand-wise estimates of carbon stocks and sequestration in the aboveground coarse wood biomass of wetland forests in the northern Pantanal, Brazil, Biogeosciences, 8, 3407–3421, doi:10.5194/bg-8-3407-2011, 2011.

Shearman, P., Bryan, J., and Laurance, W. F.: Are we approaching ‘peak timber’ in the tropics?, Biol. Conserv., 151, 17–21, 2012.

Soares-Filho, B. S., Nepstad, D. C., Curran, L. M., Cerqueira, G. C., Garcia, R. A., Azevedo Ramos, C., Voll, E., McDonald, A., Lefebvre, P., and Schlesinger, P.: Modelling conservation in the Amazon basin, Nature, 440, 520–523, 2006.

Sombroek, W.: Spatial and temporal patterns of Amazon rainfall, Ambio, 30, 388–396, 2001.

Stadtler, E.: Estimativas de biomassa lenhosa, estoque e seqüestro de carbono acima do solo ao longo do gradiente de inundação em uma floresta de igapó alagada por água preta na amazônia central, M.Sc. thesis, National Institute for Amazon Research, Brazil, 57 pp., 2007.

The New York Botanical Garden: International Plant Science Center – The C. V. Starr Virtual Hebarium, http://sciweb.nybg.org/science2/vii2.asp, 12 November 2012.

Tomasella, J., Borma, L. S., Marengo, J. A., Rodriguez, D. A., Cuartas, L. A., Nobre, C. A., and Prado, M. C. L.: The droughts of 1996–1997 and 2004–2005 in Amazonia: hydrological response in the river main stem, Hydrol. Process., 2010.

Vetter, R. E.: Untersuchungenüber Zuwachsrhythmen an tropischen Bäumen in Amazonien, PhD Thesis, University of Freiburg, 108 pp., 1995.

Wittmann, F., Schöngart, J., Montero, J. C., Motzer, T., Junk, W. J., Piedade, M. T. F., Queiroz, H. L., and Worbes, M.: Tree species composition and diversity gradients in white-water forests across the Amazon Basin, J. Biogeogr., 2006, 33, 1334–1347, 2006.

Wittmann, F., Schöngart, J., and Junk, W. J.: Phytogeography, species diversity, community structure and dynamics of central Amazonian floodplain forests, in: Amazonian floodplain forests: Ecophysiology, biodiversity and sustainable management, edited by: Junk, W. J., Piedade, M. T. F., Wittmann, F., Schöngart, J., and Parolin, P., Ecological Studies, 2010, Springer Verlag, Dordrecht, Heidelberg, London, New York, 61–102, 2010.

Worbes, M.: Growth rings, increment and age of tree in inundation forest, savannas and a mountain forest in the Neotropics, IAWA Bull. 10, 109–122, 1989.

Worbes, M.: How to measure growth dynamics in tropical trees – a review, IAWA J., 16, 337–351, 1995.

Worbes, M.: Annual growth rings, rainfall-dependent growth and long-term growth patterns of tropical trees from the Capparo Forest Reserve in Venezuela, J. Ecol., 87, 341–403, 1999.

Worbes M.: One hundred years of tree-ring research in the tropics – a brief history and an outlook to future challenges, Dendrochronologia, 20, 217–231, 2002.

Worbes, M. and Junk, W. J.: C14 dating of tropical trees, Ecology, 70, 503–507, 1989.

Yoon, J.-H.and Zeng, N.: An Atlantic influence on Amazon Rainfall, Clim. Dynam., 34, 249–264, 2010.

Zuidema, P. A., Brienen, R. J. W., and Schöngart, J.: Tropical forest warming: looking backwards for more insights, Trends Ecol. Evol., 27, 193–194, 2012.

Table 1. Geographical position, hydrology and rainfall patterns of the selected study sites. HAND (Height Above Nearest Drainage) model data indicate the elevation above the nearest drainage (Rennó et al., 2008; Nobre et al., 2011); number in parenthesis indicates the flood height of seasonally inundated forests measured in the field. SRTM (Shuttle Radar Topographic Mission) digital elevation model estimates the elevation above sea level of each plot. The Soil Water Saturation (SWS) index is explained in more detail in Table 2 (no data of the SWS is available for the plot M05.TN500). Rainfall data were obtained from the Brazilian Waters Agency (Agência Nacional de Águas – ANA).

Plot ID	Plot coordinates	SRTM (m)	HAND (m)	SWS Index	Mean annual rainfall (mm)	Length of dry season (months)
M01-TN1500	3°21′3.73″ S, 59°50′48.78″ W	35.5	1.0(1.5)	3	2300	3
M01-TN2500	3°20′55.27″ S, 59°50′14.58″ W	32.2	3.0 (5.0)	3		
M05-TN(-)500	4°36′58.05″ S, 43° 14’37.44″ W	48.9	3.3	3	2810	2
M05-TN1500	4°36′11.82″ S, 61°15′28.10″ W	50.0	2.0	2		
M08-TS2500	5°38′18.54″ S, 62°10′41.24″ W	69.4	3.4	1	2600	3
M08-TS4500	5°38′51.38″ S, 62°9′45.25″ W	66.6	3.5	2		
M11-TN1500	7°12′24.72″ S, 63°7′0.29″ W	72.8	3.8	2	2100	4
M11-TN2500	7°12′38.37″ S, 63° 6’30.52″ W	69.8	1.6	4		

Table 2. Scores for varying soil physical characteristics and water saturation (adapted from Quesada et al., 2010).

Constantly flooded; patches of stagnated water	4
Seasonally flooded; soils with high clay content and very low porosity and/or dominated by plinthite	3
Deep saturated zone (maximum high saturation of 50 cm deep); redox features	2
Deep saturated zone (maximum high of saturation > 100 cm deep); deep redox features	1
Unsaturated conditions	0

Table 3. Number of sampled and not sampled trees with DBH > 30 cm in each plot. Numbers in parenthesis indicate percentages of trees.

Plot code	Number of trees per hectare	Number of sampled trees per hectare	Number of not sampled trees per hectare
M01-1500	65	57 (88)	08 (12)
M01-2500	50	48 (96)	02 (4)
M05-(-)500	57	47 (82)	11 (19)
M05-1500	89	73 (82)	16 (18)
M08-2500	78	53 (68)	25 (32)
M08-4500	89	47 (53)	42 (47)
M11-1500	111	54 (44)	57 (56)
M11-2500	98	48 (48)	50 (52)

Table 4. Basal area per hectare for the diameter classes DBH > 30 cm and < 30 cm, mean canopy height (H, trees with DBH > 30 cm), mean wood density (ρ) with standard deviation of each plot, mean tree age(Age) and linear regression models between DBH and tree height for each module.

	Plot ID							
	M01- TN1500	M01- TN2500	M05-TN(-)500	M05- TN1500	M08- TS2500	M08- TS4500	M11- TN1500	M11- TN2500
Basal area ($m^2\ ha^{-1}$)	16	17	22	27	25	28	24	21
Mean Canopy height (m)	25 ± 4.5	24 ± 3.9	27 ± 5.0	28 ± 4.0	28 ± 5.9	25 ± 5.3	32 ± 7.9	27 ± 4.9
ρ ($g\ cm^{-3}$)	0.65 ± 0.15	0.64 ± 0.13	0.72 ± 0.14	0.71 ± 0.16	0.68 ± 0.13	0.67 ± 0.12	0.65 ± 0.14	0.67 ± 0.16
Age (yr)	90	78	106	115	121	105	123	79

	Non-linear regression models between DBH and tree height			
	M01	M05	M08	M11
N	162	145	165	158
P	< 0.01	< 0.01	< 0.01	< 0.01
R^2	0.62	0.30	0.62	0.56
Model	$H = 4.1244\ \mathrm{DBH}^{0.4755}$	$H = 6.8181\ \mathrm{DBH}^{0.3681}$	$H = 5.3026\ \mathrm{DBH}^{0.4389}$	$H = 3.899\ \mathrm{DBH}^{0.5306}$

Table 5. Mean value and standard deviation of wood density and (ρ) and mean radial increments (MRI) for tree species with five or more individuals in the study sites.

Tree species	ρ (g cm^{-3})	MRI (mm yr^{-1})
Apeiba echinata Gaertn.	0.44 ± 0.11	3.4 ± 2.4
Bertholletia excelsa Bonpl.	0.61 ± 0.04	1.6 ± 0.6
Brosimum rubescens Taub.	0.56 ± 0.08	1.9 ± 0.4
Buchenavia grandis Ducke	0.71 ± 0.11	2.2 ± 0.8
Diplotropis martiusii Benth.	0.66 ± 0.10	1.7 ± 0.1
Ecclinusa guianensis Eyma	0.69 ± 0.09	1.5 ± 0.9
Erisma bicolor Ducke	0.49 ± 0.07	2.3 ± 1.2
Eschweilera truncata A.C.Sm.	0.77 ± 0.05	1.5 ± 0.5
Eschweilera coriacea (DC.) S.A.Mori	0.81 ± 0.07	1.1 ± 0.4
Goupia glabra Aubl.	0.74 ± 0.06	2.5 ± 1.8
Licania micrantha Miq.	0.84 ± 0.06	1.4 ± 0.1
Licania oblongifolia Standl.	0.90 ± 0.05	1.3 ± 0.5
Pouteria guianensis Aubl.	0.79 ± 0.15	1.3 ± 0.5
Pouteria virescens Baehni	0.80 ± 0.13	1.3 ± 0.4
Pseudolmedia laevis (Ruiz & Pav.) J.F.Macbr.	0.70 ± 0.09	1.1 ± 0.2
Pterocarpusofficinalis Jacq.	0.77 ± 0.11	1.5 ± 0.9
Scleronema micranthum (Ducke) Ducke	0.54 ± 0.09	1.4 ± 0.4
Sapotaceae sp. 67	0.72 ± 0.09	2.2 ± 1.5

Table 6. Estimates of AGWB and C-stocks in AGWB calculated by Eqs. (2) and (3). For each estimate the error (σ_{AGWB}) is indicated. Furthermore for each plot information on aboveground coarse wood productivity (AGWBP) and carbon sequestration per hectare and year (C-sequestration) and the structural conversion factor ($\mathrm{AGWB}_{\mathrm{SCF}}$ and $\mathrm{AGWBP}_{\mathrm{SCF}}$ related to m2 basal area) are indicated. Here, $\mathrm{AGWBP}_{\mathrm{C}}$ was calculated as the sum of the mean of the productivity of all trees for the last five years, and $\mathrm{AGWBP}_{\mathrm{SCF}}$ was calculated as the sum of the mean productivity of all trees for the whole life.

	Plot ID							
	M01-TN1500	M01-TN2500	M05-TN(-)500	M05-TN1500	M08-TS2500	M08-TS4500	M11-TN1500	M11-TN2500
Eq. (2)								
AGWB ($\mathrm{Mg\,ha^{-1}}$)	134	132	222	281	266	269	289	199
$\mathrm{AGWB}_{\mathrm{SCF}}$ ($\mathrm{Mg\,m_{BA}^{-2}}$)	8.4	7.6	10.1	10.4	10.8	9.7	12.1	9.7
σ_{AGWB} ($\mathrm{Mg\,ha^{-1}}$)	4.0	4.0	4.7	5.0	5.1	3.8	15.2	6.0
C-stock ($\mathrm{Mg\,ha^{-1}}$)	61	59	101	128	120	122	130	90
$\mathrm{AGWBP}_{\mathrm{c}}$ ($\mathrm{Mg\,ha^{-1}\,yr^{-1}}$) (Eq. 10)	4.2	3.5	6.5	6.8	6.1	6.9	6.4	7.1
$\mathrm{AGWBP}_{\mathrm{m}}$ ($\mathrm{Mg\,m_{BA}^{-2}\,yr^{-1}}$) (Eq. 11)	0.13	0.11	0.13	0.10	0.10	0.10	0.11	0.14
C-sequestration ($\mathrm{Mg\,ha^{-1}\,yr^{-1}}$)	1.9	1.6	3.0	3.1	2.7	3.1	2.9	3.2
Eq. (3)								
AGWB ($\mathrm{Mg\,ha^{-1}}$)	145	142	240	304	287	290	312	215
$\mathrm{AGWB}_{\mathrm{SCF}}$ ($\mathrm{Mg\,m_{BA}^{-2}}$)	9.0	8.2	10.9	11.2	11.6	10.4	13.1	10.5
σ_{AGWB} ($\mathrm{Mg\,ha^{-1}}$)	4.3	4.4	5.0	5.4	5.6	4.1	16.4	6.5
C-stock ($\mathrm{Mg\,ha^{-1}}$)	65	64	109	138	130	131	141	98
$\mathrm{AGWBP}_{\mathrm{c}}$ ($\mathrm{Mg\,ha^{-1}\,yr^{-1}}$) (Eq. 10)	3.9	3.3	6.0	6.3	5.5	5.8	5.9	6.4
$\mathrm{AGWBP}_{\mathrm{mean}}$ ($\mathrm{Mg\,m_{BA}^{-2}\,yr^{-1}}$) (Eq. 11)	0.14	0.13	0.14	0.11	0.12	0.12	0.13	0.15
C-sequestration ($\mathrm{Mg\,ha^{-1}\,yr^{-1}}$)	1.8	1.5	2.7	2.9	2.5	2.6	2.7	2.9

Table 7. Chemical and physical soil properties obtained from 30 cm depth composite soil samples for each study site.

Plot_id	Clay (%)	Coarse sand (%)	Total sand (%)	Fine sand (%)	Silt (%)	Fe^+ ($\text{mg g}_{\text{soil}}^{-1}$)	P ($\text{mg g}_{\text{soil}}^{-1}$)
M01-1500	12.2	0.8	19.0	18.2	68.6	224.9	6.3
M01-2500	27.8	1.0	16.4	15.4	55.7	316.2	6.3
M05-(-)500	15.1	29.6	46.8	17.2	37.9	195.8	2.0
M05-1500	20	1.4	22.8	21.4	57.1	312.5	3.1
M08-2500	17	1	19.7	18.7	63.2	388.8	1.4
M08-4500	14.6	0.7	17.9	17.2	67.5	139.6	2.0
M11-1500	28.4	26.8	58.3	31.5	13.2	136.2	2.2
M11-2500	19.7	0.4	20.9	20.4	59.3	66.7	2.8

Table 8. Comparison between estimates of AGWB (in Mg ha^{-1}) and AGWBP (in $\text{Mg ha}^{-1}\,\text{yr}^{-1}$) of old-growth forests from this study, with estimates from floodplain forests (igapó, várzea) and non-flooded sites (paleovárzeas, terra firme) from other studies. The studies of Stadtler (2007), Oliveira (2010) and Schöngart et al. (2010) applied for the estimates of AGWB and AGWBP Eqs. (2) and (3), while Chambers et al. (2001) and Malhi et al. (2004, 2006) use allometric models with only one (diameter) and two independent variables (diameter, wood density), respectively. SFC (in $\text{Mg m}_{\text{BA}}^{-2}$) is the structural conversionfactor relating AGWB to 1 square meter basal area (BA). The results of other studies that present their values in MgC were doubled to correspond to biomass.

	Area	SFC ($\text{Mg m}_{\text{BA}}^{-2}$)	AGWB (Mg ha^{-1})	AGWBP ($\text{Mg ha}^{-1}\,\text{yr}^{-1}$)
This Study	Purus-Madeira interfluvial region	10.8 ± 1.6	252 ± 75	5.6 ± 1.1
Schöngart et al. (2010)	Central Amazonian várzea floodplains	8.8 ± 0.4	235 ± 07	5.7 ± 0.7
Chambers et al. (2001)	Central Amazonian terra firme forests	–	324 ± 36	4.1 ± 0.7
Malhi et al. (2004, 2006)	South Western Amazonian terra firme forests, Peru	10.1 ± 0.6	270 ± 40	7.0 ± 1.5
Stadtler (2007)	Central Amazonian igapó floodplain	8.9 ± 1.6	238 ± 29	3.6 ± 1.2
Oliveira (2010)	Paleovárzeas	7.2 ± 0.2	192 ± 14	5.4 ± 0.7

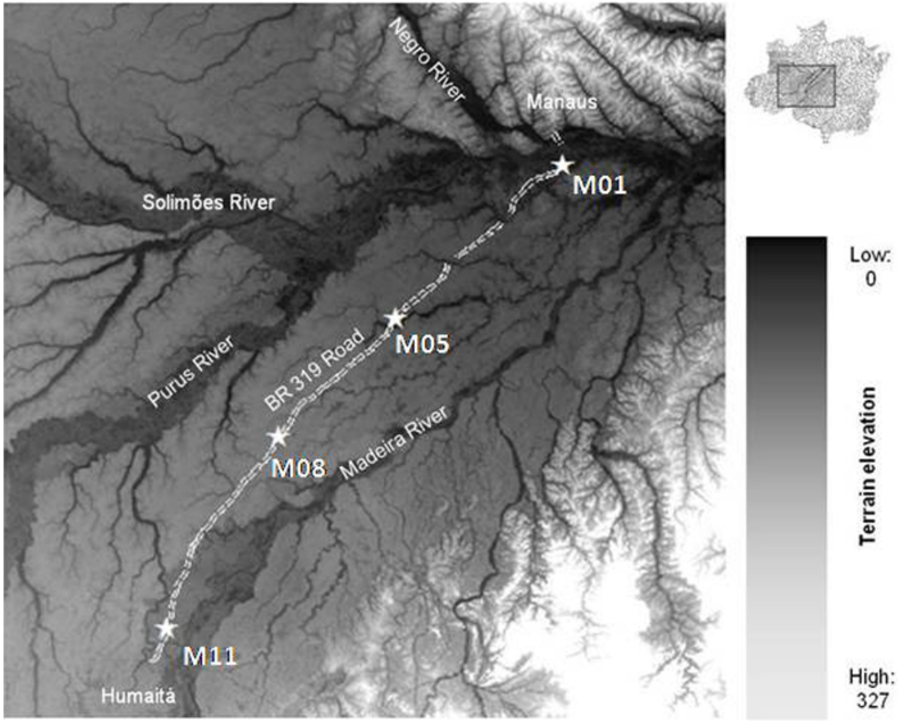

Fig. 1. Map of the Purus-Madeira interfluvial area that is crossed by the BR-319 Highway. The study sites are indicated by white asterisks. All study sites are sampling modules (*M*) of the PRONEX Project Rapid Assessment for Long Duration Ecological Projects (RAPELD).

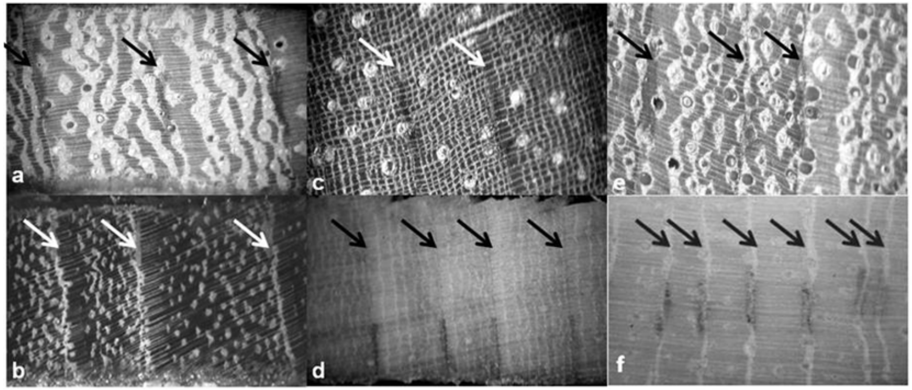

Fig. 2. Examples of distinct tree rings. The classification of wood anatomy of the tree rings is described following Worbes (2002): **(a, b)** Parenchyma bands limiting ring boundaries and vessel size/distribution variation from earlywood to latewood; **(c, d)** alternating fiber and parenchyma bands, large in the earlywood and narrow in the latewood; **(d, e)** parenchyma bands defining the ring boundaries.

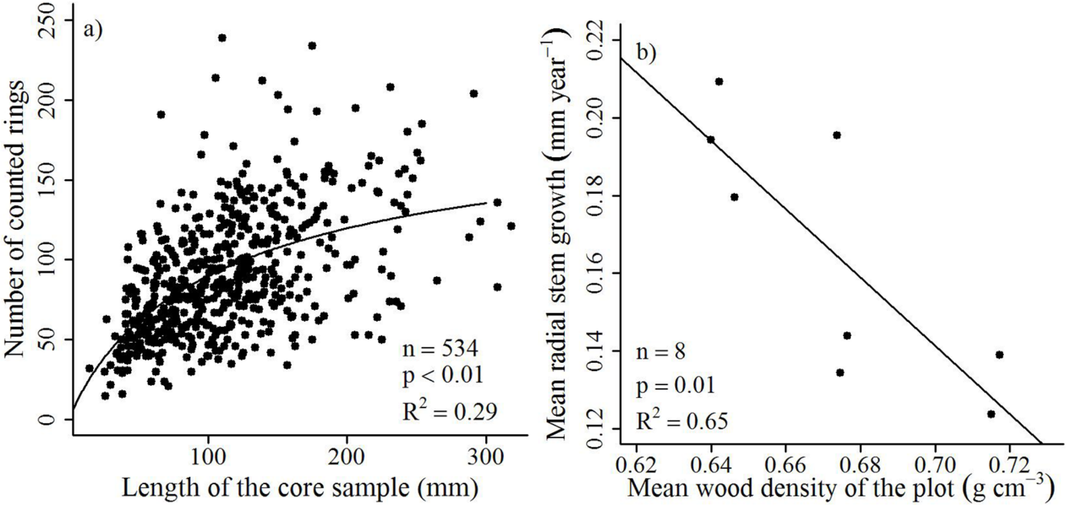

Fig. 3. Significant non-linear relationship between the number of counted rings and length of the core samples for all analyzed trees with distinct growth rings and **(a)** significant relationship between estimated mean radial stem growth and mean wood density of 1 ha plots **(b)**.

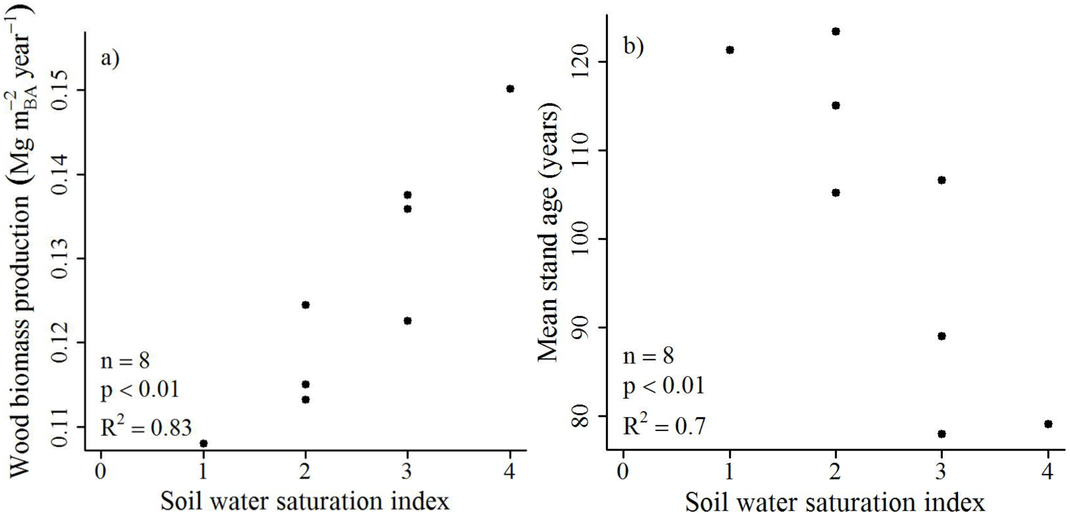

Fig. 4. Significant relationship between soil water saturation index and **(a)** mean aboveground wood biomass productivity ($AGWBP_m$, see Eq. 11), and **(b)** plot mean tree age.

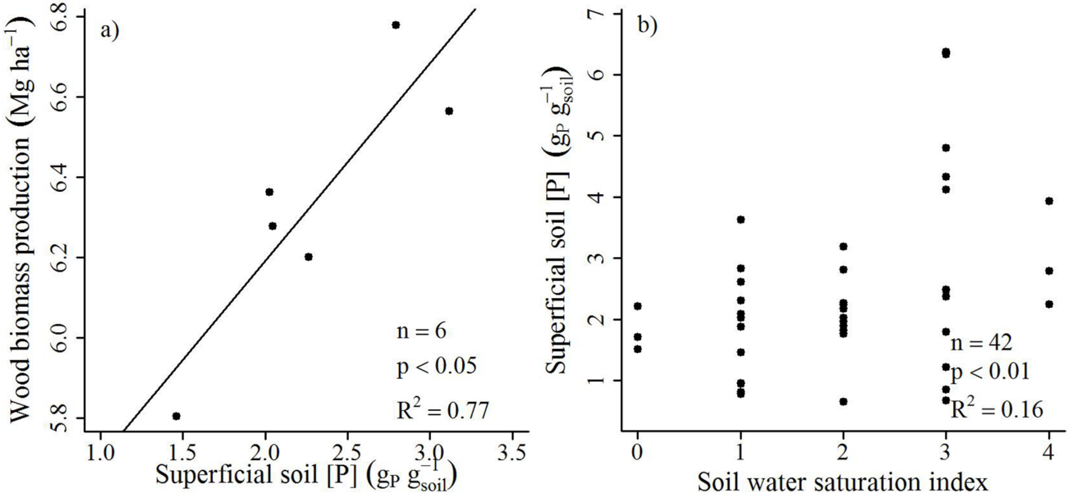

Fig. 5. Significant relationship between soil superficial available phosphorus and total aboveground wood productivity ($AGWBP_c$, see Eq. 10) **(a)** and significant relationship between regional variation of soil superficial available phosphorus and soil water saturation index **(b)**.

Title Page
Abstract
Introduction
Conclusions
References
Tables
Figures
◀▌ ▐▶
◀ ▶
Back
Close
Full Screen / Esc
Printer-friendly Version
Interactive Discussion